

Glycomic Signature of Mouse Embryonic Stem Cells During Differentiation

Rania Harfouche^{1,2*}, Somak Ray³, Melinda Sanchez¹, Ushashi Dadwal^{1,2}, Steven R Head⁴, Aaron Goldman^{1,2} and Shiladitya Sengupta^{1,2,5,6*}

¹BWH-HST Center for Biomedical Engineering, Harvard Medical School, Cambridge, USA

²Harvard-MIT Division of Health Sciences and Technology, Harvard Medical School, Cambridge, USA

³The Barnett Institute, Boston, USA

⁴DNA Array Core Facility, The Scripps Research Institute, La Jolla, USA

⁵Channing Laboratory, Department of Medicine, Brigham and Women's Hospital, Harvard Medical School, Cambridge, USA

⁶Dana Farber Cancer Institute, Boston, USA

Abstract

Background: The glycome has emerged as a key regulator of cell fate, partly through its ability to potentiate the action of numerous signaling pathways. We recently demonstrated that a sulfated component of the glycome plays a critical role in promoting the differentiation of embryonic stem cell (ESC)-derived embryoid bodies by modulating downstream growth factors, such as the insulin-like growth factor (IGF) signaling axis. However, the exact components of the glycome which promote ESC differentiation versus stemness remain uncharacterized, due to the lack of a rapid, simple and easily quantifiable methodology. As a proof-of-concept in this study, we utilized a custom-made glycoarray in combination with bioinformatics and molecular biology tools in order to uncover novel glyco-signatures underlying ESC differentiation in an embryoid body model. A better elucidation of the glycomic transcriptomal signature underlying ESC differentiation would allow us to better manipulate these cells towards a desired lineage.

Method: We used a custom-designed Affymetrix microarray, the Glycogene-chip, to screen the transcriptome of differentiating embryoid bodies versus that of undifferentiated ESC. In conjunction with gene ontology, pathway analyses, real-time PCR and immunoblotting, we validated the involvement of the IGF family, and furthermore, uncovered novel differentially regulated genes belonging to the glycoprotein (Angiopoietin-1 and Angiopoietin-like members), sulfotransferase, sulfatase and glycosyltransferase families.

Conclusion: These results suggest that the Glycogene-chip, in conjunction with the embryoid body model, provides a fast and reliable tool to uncover novel glycomic signatures that are critical to maintain ESC stemness versus differentiation. In turn, this will allow us to understand the mechanisms governing ESC fate, bringing us one step closer towards finding a new paradigm for the regenerative medicine field.

Keywords: Embryonic stem cells; Differentiation; Glycome; Microarray; Angiopoietin

Abbreviations: ABIN: A20 Binding Inhibitor of NF-kappaB; AN: Analyze Networks; ANGPT: Angiopoietin; ANGPTL: Angiopoietin-like; AP: Activator Protein; BRB: Biometric Research Branch; CBF: Core-Binding Factor; CFG: Consortium for Functional Glycomics; CHST: Carbohydrate-Specific Sulfotransferase; DCN: Decorin; ESC: Embryonic Stem Cells; EXTL: Exostoses (multiple)-like; FGF: Fibroblast Growth Factor; FKHR: Forkhead Transcription Factor; GO: Gene Ontology; GOBP: Gene Ontology Biological Process; IGF: Insulin-like Growth Factor; IGFBP: IGF-binding protein; ITGA: Integrin Alpha; GALNS: Galactosamine (N-acetyl)-6-sulfate Sulfatase; HS3ST: Heparan Sulfate (glucosamine) 3-O-sulfotransferase; LIF: Leukemia Inhibitory Factor; PDGF: Plated-Derived Growth Factor; LUM: Lumican; PECAM: Platelet Endothelial Cell Adhesion Molecule; SP: Specificity Protein; ST3GAL: Beta-galactoside alpha-2,3-sialyltransferase; STAT: Signal Transducer And Activator Of Transcription; TGF: Transforming Growth Factor; NDST: N-deacetylase/N-sulfotransferase; TIE: Tyrosine Kinase with Immunoglobulin-like and EGF-like Domains; SULF: Sulfatase. VCAM: Vascular Cell Adhesion Molecule

Background

Within the past decade, glycomics has emerged as a key modulator of cellular function and homeostasis. As such, glycosylation of protein and lipids constitutes one of the most common post-translational modifications in eukaryotes, resulting in modulation of key developmental functions, including innate immunity, signal transduction and cell differentiation [1,2]. These pleiotropic effects of the glycome are mainly mediated by the presence of a wide range of glyco-enzymes and their respective isoforms, as well as by the fact that a single glyco-conjugate can simultaneously modulate the activity of

numerous growth factors/receptor complexes due to the complexation of various factors onto one conjugate [3,4]. Glyco-conjugates are therefore more potent determinants of cell fate as opposed to the action of a single growth factor/receptor pair.

Despite these predominant roles of the glycome in governing cell fate, its underlying mechanisms of action remain largely uncharacterized, especially in the stem cell field. Effectively, the mechanisms which act as a switch between stem cell proliferation *versus* differentiation remain the subject of extensive studies, and harnessing these mechanisms would have immense potential in the field of regenerative medicine. Most studies thus far have focused on the roles of various growth factors to induce stem cell renewal or to promote their differentiation into selective lineages [5,6]. The few studies which have investigated glycome-related changes governing stem cell fate have used either lectin or antibody arrays which monitor specific glycoprotein-receptor interactions [7,8]. These studies have all encountered similar limitations, including false negatives and

***Corresponding author:** Rania Harfouche, BWH-HST Center for Biomedical Engineering, Harvard Medical School, 65 Landsdowne Street, Cambridge, MA 02139, USA, E-mail: rharfo@gmail.com

Shiladitya Sengupta, BWH-HST Center for Biomedical Engineering, Harvard Medical School, 65 Landsdowne Street, Cambridge, MA 02139, USA

Received July 22, 2013; **Accepted** August 21, 2013; **Published** August 24, 2013

Citation: Harfouche R, Ray S, Sanchez M, Dadwal U, Head SR, et al. (2013) Glycomic Signature of Mouse Embryonic Stem Cells During Differentiation. Cell Dev Biol 2: 120. doi:10.4172/2168-9296.1000120

Copyright: © 2013 Harfouche R, et al. This is an open-access article distributed under the terms of the Creative Commons Attribution License, which permits unrestricted use, distribution, and reproduction in any medium, provided the original author and source are credited.

analyses artefacts (as many lectins have low affinity for their ligands and glyco-antibodies are scarce), growth factor/cytokine redundancy and irreproducibility.

We were one of the first groups to report that the glycome is a critical modulator of embryonic stem cell (ESC) fate [9]. Specifically, using an embryoid body model, we demonstrated that a sulfated subset of the glycome (the heparan sulfate glycosaminoglycans) directed ESC differentiation towards the mesodermal lineage, partly through modulation of the insulin-like growth factor (IGF) pathway [9,10]. Similarly, recent studies imply that the glycome is dynamically regulated during (embryonic or precursor) stem cell differentiation [11,12]. The exact players involved in ESC differentiation *versus* stemness, however, remain uncharacterized. A main reason for this lacuna remains the lack of a rapid, simple and easily quantifiable screening methodology to probe the ESC glycome.

In this study, we took advantage of a custom-designed oligonucleotide array developed and annotated by the Consortium for Functional Glycomics (CFG), which specifically probes for glycomic transcripts, in order to screen for the glyco-specific transcriptome underlying ESC differentiation [13-16]. As a proof-of-concept, we employed a well-established embryoid body model of ESC differentiation, which recapitulates embryonic development *in vivo*, and compared its transcriptomal profile over time to that of undifferentiated ESC using bioinformatic analyses. We uncovered novel genes implicated in ESC differentiation *versus* stemness and validated these findings by real-time PCR and immunoblotting. Some of the genes of interest included glycoproteins, namely the Angiopoietin (ANGPT) and Angiopoietin-like (ANGPTL) families, as well as sulfotransferases, sulfatases and glycosyltransferases.

Materials and Method

Materials

The RNeasy kit was obtained from Qiagen (Valencia, CA), whereas the iScript cDNA synthesis kit, iTaq SYBR Green Supermix and MyIQ PCR cyclers were all from Bio-Rad Laboratories (Hercules, CA). All primers were obtained from Integrated DNA Technologies (Coralville, IA). Tie-2 receptor antibodies (sc-324, dilution 1:250) were purchased from Santa Cruz Biotechnology (Santa Cruz, CA).

Stem cell culture

A murine embryonic stem cell (ES) line derived from a 129 substrain (9TR#1) was purchased from ATCC (Rockville, MD). ES were maintained undifferentiated on gelatin-coated plates using a growth medium consisting of L-glutamine-containing DMEM, 0.1 mM non-essential amino acids, 0.1 mM sodium pyruvate, 0.1 mM 2-mercaptoethanol, all from Invitrogen (Carlsbad, CA), as well as 1000 U/ml LIF (Chemicon Inc., Temecula, CA) and 15% fetal bovine serum (HyClone, Logan, UT). Differentiation into embryoid bodies was induced by removing LIF from the medium and seeding the cells on ultra-low attachment 100mm dishes (Corning, Lowell, MA). Cells were imaged in real-time using bright field microscopy (Nikon Eclipse TE-2000 U).

RNA preparation and quality control

ES were differentiated on ultra-low attachment dishes to induce embryoid body formation. Quadruplet dishes were harvested for RNA extraction and the same samples subjected to real-time PCR and Glycogene-chip analyses. Undifferentiated ES were considered as Day 0 control. At indicated time-points, cells were harvested and

total RNA extracted using the Qiagen RNeasy Mini Kit, following the manufacturer's instructions. All samples were treated with DNaseI to prevent genomic DNA contamination. Quantification and purity of total RNA was assessed by A260/A280 absorption using a micro-volume plate reader (Biotek, Winooski, VT). RNA quality was further investigated by the CFG core E facility using the Agilent Technologies 2100 Bioanalyzer using the RNA 6000 Nano LabChip (Santa Clara, CA) and was deemed to be excellent.

Glycogene-chip oligonucleotide array hybridization

GLYCOv4, referred to herein as Glycogene-chip, is a custom-made Affymetrix oligonucleotide array (Affymetrix, Santa Clara, CA) designed for the Consortium for Functional Glycomics (GFC) at the Scripps Research Institute (La Jolla, CA) [13]. Information is available online at: <http://www.ncbi.nlm.nih.gov/geo/query/acc.cgi?acc=GPL11098>. This array includes probes for ~1246 murine probe-ids related to mouse glycome and developmental genes, where each gene is represented by 11 probe pairs. Unlike commercial oligonucleotide microarrays, it includes genes not currently represented, including glycosyltransferases, carbohydrate-binding proteins and proteoglycans. RNA (0.5 µg) from quadruplet samples was amplified using the Ambion Message Amp II Biotin Enhanced Single Round aRNA Amplification Kit (Agilent Technologies) and hybridized overnight to the GLYCOv4 array using a standard Affymetrix protocol, as previously described [17]. Glycogene-chips were scanned using the Affymetrix GeneChip Scanner 3000 7G with default settings and a target intensity of 250 for scaling.

Glycogene-chip data analysis

The dendrogram was generated by unsupervised hierarchical clustering using Biometric Research Branch (BRB) ArrayTools, as previously described [13]. Acquired probe level data was normalized using the RMA Express 1.0 with quantile normalization, median polish and background adjustment. Differential expression between transcripts was generated using the Limma package in the R software [18]. The fold changes and standard errors were estimated by fitting a linear model for each gene and empirical Bayes smoothing was applied to the standard errors. Results are presented as fold induction, and were calculated using the moderated t-statistic, the p-value, and the adjusted p-value, the latter being generated using the Benjamini and Hochberg's method. The transcripts identified as differentially expressed were those with adjusted p-value < 0.1 and fold change > 1.4. These analyses were performed by the GFC. The Gene Ontology Biological Process (GOBP) terms were retrieved using the Bioconductor [19] packages 'biomaRt' and 'GO.db' and GeneGo Metacore (www.genego.com) biological pathway analysis tool [20].

Biological chart and pathway analyses

The Cytoscape (<http://cytoscape.org/>) plugin ClueGO [21] was used to generate functionally-grouped molecular function network charts (26.03.2012, cutoff of $Q \leq 0.00001$ level of significance). Significance for enrichment and depletion of groups and terms was calculated by a two-sided hypergeometric test with a Bonferroni correction for multiple testing. The differentially expressed genes were subjected to biological pathway analysis from the GeneGo Metacore software (www.genego.com) using Analyze Networks (AN) algorithm with default settings [20]. Enrichment analysis was performed by mapping gene IDs of the dataset onto gene IDs in entities of built-in functional ontologies represented in MetaCore by pathway maps. Gene networks were then segregated into their respective cellular compartments. The gene content of the uploaded files is used as the input list for generation

of biological networks using Analyze Networks (AN) algorithm with default settings. This is a variant of the shortest paths algorithm with main parameters of relative enrichment with the uploaded data, and relative saturation of networks with canonical pathways. These networks are built on the fly and are unique for the uploaded data. In this workflow the networks are prioritized based on the number of fragments of canonical pathways on the network.

Real-time PCR

RNA was extracted from cells using the RNeasy kit and reverse-transcribed with the High-Capacity cDNA Reverse Transcription kit, according to the manufacturer's instructions. The resulting cDNA was subjected to SYBR Green real-time PCR using primers designed to amplify ANGPT-1, ANGPTL-2, -4, -6, CHST-1, EXTL-1, GALNS, HS3ST-1, NANOG and SULF-1. GAPDH was used as the endogenous control [22]. Primers were designed to span exon-exon boundaries using the Universal ProbeLibrary Assay Design Center (Roche Applied Science) and. Normalized reporter (Rn) values were calculated using the threshold cycle value (C_T) for each gene, as follows:

$$Rn = 2^{-\Delta\Delta C_T}, \text{ where } \Delta\Delta C_T = \text{average } C_{T\text{target}} - \text{average } C_{T\text{experimental control}}$$

Results were expressed as mean±SEM of quadruplicate samples and repeated at least twice. Statistical comparisons were obtained using one-way ANOVA, followed by the Newman-Keuls test. Probability (p) values less than 0.05 were considered significant.

Immunoblotting

Cells were washed twice with PBS and directly lysed in 3X loading buffer containing 12% sodium dodecyl sulfate, 15% 2-mercaptoethanol, 1 mM sodium orthovanadate and protease inhibitor cocktail tablets from Roche Applied Science. Cells were further homogenized by passing the lysates 3 times through an insulin needle. Samples were then heated for 5 min at 100°C and equal amounts loaded onto tris-glycine SDS-polyacrylamide gels. Proteins were electrophoretically transferred onto polyvinylidene difluoride membranes, blocked for 1 h with 5% non-fat dry milk, and subsequently incubated overnight at 4°C with primary antibodies directed against phosphor-Tie-2 receptor. Proteins were detected using horseradish peroxidase-conjugated anti-rabbit secondary antibodies and Lumi-LightPLUS Western Blotting Substrate (Roche Applied Science). The blots were developed using GeneSnap and optical densities off the protein bands quantified using GeneTools (both from SynGene, Frederick, MD). Predetermined molecular weight standards were used as markers. Proteins were normalized against total Tie-2. Statistical comparisons of 3 immunoblots were obtained using one-way ANOVA, followed by the Newman-Keuls test. Probability (p) values less than 0.05 were considered significant.

Results and Discussion

A glycome-selective microarray shows specific clustering during ESC differentiation

We used a standard model of ESC differentiation into embryoid bodies, which spontaneously recapitulates the three stages of *in vivo* embryonic development, namely mesoderm, endoderm and ectoderm [9,23,24]. These cells were maintained in suspension for 5 to 15 days on ultra-low adherent wells and in the absence of leukemia inhibitory factor (LIF) (Figure 1A). In contrast, ESC maintained in the adherent state and in the presence of LIF, represented as Day 0, served as the undifferentiated control, before gastrulation has occurred. Cells maintained for 5 days differentiate into cystic, symmetrical

embryoid bodies, representing the beginning of the gastrulation stage [9,24,25]. Day 7 represent the organogenesis stage, beginning with the development of the cardiovascular system, whereas Day 10 and thereafter are characterized by a high proportion of endodermally-derived cell types and neurogenesis [9,24]. This model hence allows us to accurately monitor glycome-selective changes occurring during all stages of development.

RNA was extracted and labeled from these ESC, with each time-point represented by quadruplicate experimental groups. Following microarray hybridization, gene expression patterns were analyzed using unsupervised hierarchical cluster analysis in order to assess experimental reproducibility and uncover general clustering patterns. The resulting dendrogram (Figure 1B) demonstrates excellent sample reproducibility among each quadruplicates, as shown by the short branches between them, which was further corroborated by quality assessment parameters (results not shown). In addition, days 0 and 5 clustered close together, as did days 10 and 15. There was a clear separation between days 0 and 5 from the rest of the experimental time-points, reflecting clear differences in the glycome expression profiles as the ESC differentiated, as expected from the embryoid body model [9,23,24].

A more detailed investigation of the differential glycomic profile during ESC differentiation was investigated using the Venn diagram, which allowed us to focus on two groups for subsequent analyses. Figure 1C shows that 180 overlapping transcripts changed significantly between all time-points (omitting Day 5), indicating developmentally-conserved roles of the glycome throughout differentiation. We focused on these 180 genes for the first investigation. The number of genes that were unique to distinct time-points, with respect to Day 0, were as follows: 111 genes for Day 15, 18 genes for Day 10, 28 genes for Day 7 and 5 genes for Day 5. Hence, the Day 15 time-point would allow us to uncover the most glycome-related changes underlying ESC differentiation. Since, based on the dendrogram of Figure 1A, days 15 and 10 clustered close together, we decided to also focus on the subset of genes (70) overlapping in only these two time-points, for a total of 181 genes for the second investigation. Since there were the less differences between Day 5 *versus* Day 0 using this array, we did not use this time-point for subsequent analyses. This is not to imply a lack of transcriptomal changes between both time-points, but since we're using a focused microarray that doesn't include most of the genome, subtle differences might be masked, as indicated by the dendrogram of Figure 1B.

ESC exhibit a distinct glycomic transcriptomal signature during differentiation

Firstly, we focused on the upregulated (top 75, Table 1) and downregulated (69, Table 2) genes, omitting housekeeping genes, which significantly overlapped between all time-points. Transcripts identified as differentially expressed were those with adjusted p-value < 0.1 and fold change > 1.4. Results were annotated using gene ontology (GO) biological processes with fold changes tabulated using Day 0 as the denominator. The complete results from the list of the 180 transcripts are available upon request.

In order to correlate the expression profiles occurring during ESC differentiation into biologically-relevant data, we visualized the GO molecular function related to the 180 overlapping transcripts using ClueGO in Cytoscape (Figure 2). Figure 2A shows the resulting annotation network showing significant GO groups that were upregulated between all time-points, as depicted by 5 major functional

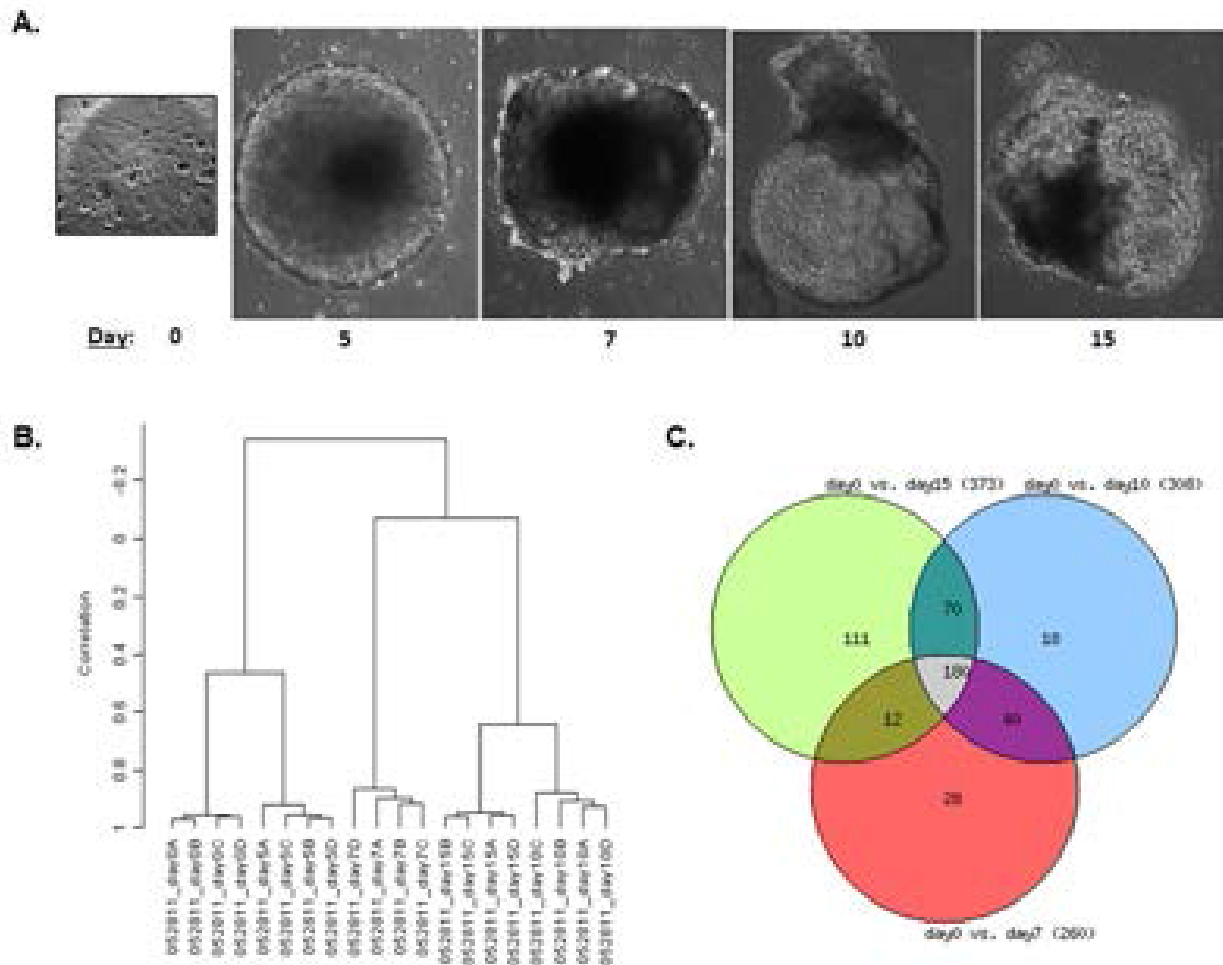


Figure 1: Dendrogram and Venn diagram of glycogene expression in differentiating embryonic stem cells (ESC). (A) Representative model of ESC differentiation relative to Day 0 taken in real-time by light microscopy. (B) The dendrogram was constructed using centered correlation and average linkage. The four biological replicates are shown for each differentiation time-point (days 5, 7, 10 and 15), with Day 0 representing undifferentiated ESC. (C) Venn diagram reveals 260, 308 and 373 regulated transcripts between undifferentiated ESC (Day 0) and ESC differentiated for 7, 10 and 15 days, respectively, whereas 180 transcripts overlapped between all time-points (7, 10 and 15) relative to Day 0. The comparisons used thresholds of adjusted p-value < 0.10 and magnitude fold change >1.4.

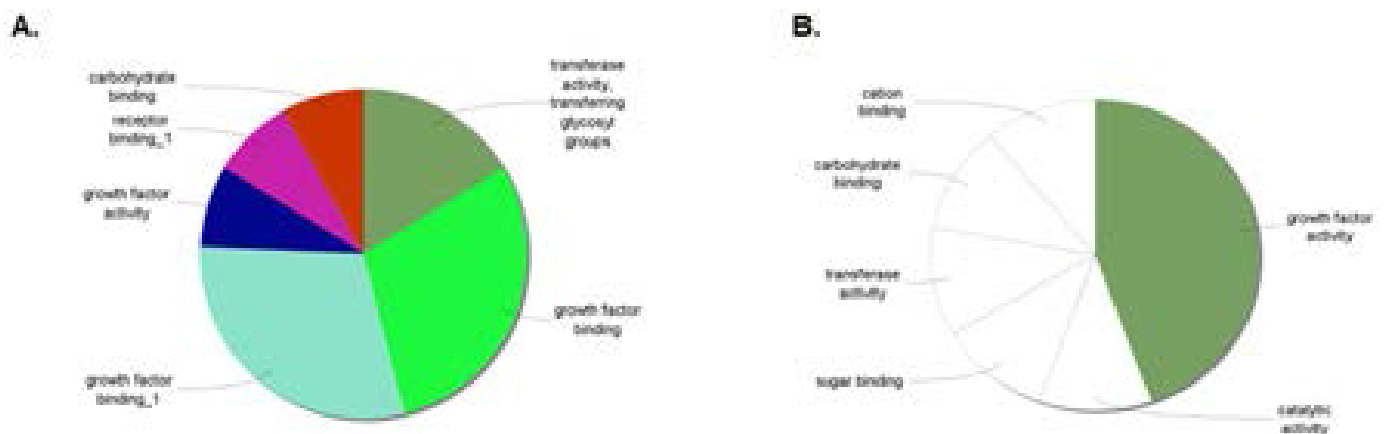


Figure 2: Classification of the 180 transcripts which significantly overlapped between all time-points of differentiating ESC versus Day 0. Molecular functional annotation network overview chart of the 180 upregulated (A) and downregulated (B) transcripts, which were created using ClueGO in Cytoscape.

themes: (1) growth factor binding; (2) transferase activity-transferring glycosyl groups; (3) carbohydrate binding; (4) receptor binding and (5) growth factor activity. Transcripts identified as differentially expressed were those with adjusted p-value < 0.1 and fold change > 1.4. Top regulated transcripts (with fold changes > 10 across at least one time-point) included members of the fibroblast growth factor (FGF), plated-derived growth factor (PDGF) and transforming growth factor families (TGF) families (Table 1). These transcripts have already been shown to play integral roles in promoting ESC differentiation [24,26,27]. As such, the top regulated transcript, FGF-8, has been implicated in priming mouse ESC towards neurogenesis [28]. Interestingly, several members of the insulin-like growth factor family (IGF) were highly upregulated in differentiating embryoid bodies, a finding previously demonstrated by our group [9,10]. These findings validate the accuracy of combining the Glycogene-chip and embryoid body models and justify their uses in this study. Although the Glycogene-chip focuses on glycomic genes, it also includes a large set of growth/developmental-related transcripts which serve as internal controls, thus explaining the high proportion of

regulated growth factor/receptor genes herein obtained. In the realm of using the Glycogene-chip to uncover novel roles of the glycome during ESC differentiation, we focused on several glyco-modifying transcripts that were upregulated to a lesser extent, including sulfatases (SULFs), sulfotransferases (CHST-1 and -2) and the glycoprotein ANGPTL-2.

The main GO theme that was downregulated was growth factor activity, with the top regulated transcript being fibroblast growth factor-4 (FGF-4, 14.29-fold) (Figure 2B and Table 2). FGF-4 expression was recently shown to positively correlate with the stemness transcription factor Nanog (Figure 3C) [29]. In addition, 5 themes that were not grouped involved catalytic activity, sugar binding, transferase activity, as well as carbohydrate and carbon binding. Altogether, these results indicate that a precise fine-tuning of growth factors is necessary to modulate ESC fate. Table 2 shows the downregulated overlapping transcripts. Besides FGF-4, main downregulated genes included members of the platelet endothelial cell adhesion molecule (PECAM) family, with up to 6.25-fold reduction at Day 10. It's also interesting that carbohydrate-specific sulfotransferase (CHST) family members

Down Regulated Genes	Biological Processes	Gen Bank ID	Day 7 vs Day 0	Adj. P. Val	Day 10 vs Day 0	Adj. P. Val	Day 15 vs Day 0	Adj. P. Val
FGF4	chondroblast differentiation	NM_010202	0.15	8.68E-20	0.07	4.34E-23	0.07	5.37E-23
MANBA	glycoprotein catabolic process	NM_27288	0.18	6.65E-19	0.11	5.02E-21	0.15	1.21E-19
PECAM1	positive regulation of tyrosine phosphorylation of Star5 protein	NM_001032378	0.18	4.07E-17	0.16	7.56E-18	0.23	2.61E-16
LGALS6	induction of programmed cell death	NM_010707	0.2	3.02E-16	0.1	1.84E-19	0.09	1.21E-19
ICAM1	response to sulfur dioxide	NM_010493	0.21	3.03E-19	0.16	1.33E-20	0.11	2.38E-22
FGF18	endochodral ossification	NM_008005	0.24	1.30E-15	0.29	1.24E-14	0.51	1.07E-09
HBEGF	positive regulation of keratinocyte migration	NM_010415	0.29	2.53E-15	0.4	5.82E-13	0.41	6.17E-13
ANGPTL4	triglyceride homeostasis	NM_020581	0.32	3.04E-16	0.21	3.81E-19	0.24	1.89E-18
BMP8 B	ossification	NM_007559	0.32	3.11E-15	0.29	5.72E-16	0.26	8.53E-17
PDGF A	positive regulation of mesenchymal cell proliferation	NM_008808	0.33	2.38E-15	0.36	1.17E-14	0.27	6.30E-17
MCAM	vascular wound healing	NM_023061	0.33	3.95E-16	0.41	1.26E-14	0.42	2.19E-14
MANBA	glycoprotein catabolic process	uc008rlu	0.34	1.56E-12	0.25	8.20E-15	0.23	2.23E-15
RBPJ	positive regulation of transcription of Notch receptor target	NM_009035	0.39	4.66E-16	0.4	4.97E-16	0.39	2.23E-16
PTCH2	skin development	NM_008958	0.41	4.34E-12	0.35	1.53E-13	0.32	3.04E-14
GLB1	galactose catabolic process	uc009rxh	0.41	1.03E-15	0.44	4.54E-15	0.45	4.03E-15
GDF3	somite rostral/caudal axis specification	NM_008108	0.42	1.56E-12	0.28	1.06E-15	0.26	1.54E-16
LGALS3	extracellular matrix organization	NM_010705	0.42	2.43E-10	0.26	3.32E-14	0.24	8.50E-15
CSF1	positive regulation of macrophage derived from cell differentiation	NM_007778	0.45	2.16E-14	0.44	1.02E-14	0.42	2.31E-15
B3GNT7	protein glycosylation	NM_145222	0.46	2.68E-09	0.26	4.52E-14	0.21	2.26E-15
GCNT2	metabolic process	NM_133219	0.46	9.37E-09	0.38	1.26E-10	0.61	5.88E-06
PMM1	mannose biosynthetic process	NM_013872	0.47	2.77E-13	0.25	2.47E-18	0.21	1.53E-19
VEGFC	positive regulation of protein autophosphorylation	NM_009506	0.47	5.57E-15	0.67	6.69E-10	0.58	2.78E-12
PMM1	mannose biosynthetic process	uc007wxu	0.47	2.52E-12	0.26	2.00E-17	0.2	6.45E-19
B3GNT2	sensory perception of smell	NM_016888	0.48	1.16E-10	0.36	1.77E-13	0.2	2.14E-15
NGF	positive regulation of protein autophosphorylation	NM_013609	0.48	2.01E-11	0.48	1.63E-11	0.46	3.13E-12
CAPN1	protein autoprocessing	uc008ggk	0.49	4.00E-09	0.49	2.92E-09	0.42	9.50E-11
HSPG2	nuclear-transcribed m-RNA catabolic process, nonsense mediated decay	uc008vjf	0.5	6.51E-11	44	1.77E-12	0.4	1.40E-13
CHST6	keratan sulfate biosynthetic process	NM_019950	0.5	4.41E-10	0.48	9.39E-11	0.56	5.21E-09
BMP8A	ossification	NM_007558	0.51	1.41E-11	0.41	3.83E-14	0.39	1.33E-14
CSF1	positive regulation of macrophage derived from cell differentiation	NM_007778	0.53	1.07E-11	0.54	1.51E-11	0.52	3.87E-12
IL17B	neutrophil chemotaxis	NM_019508	0.53	6.83E-11	0.45	8.17E-13	0.42	1.53E-13
CSF1	positive regulation of macrophage derived from cell differentiation	uc008qxm	0.53	1.82E-11	0.54	2.22E-11	0.57	1.05E-10
SLC35B2	positive regulation of I-kappaB kinase/NF-kappaB cascade	uc008cqw	0.54	4.43E-12	0.43	7.30E-15	0.35	6.71E-17
GDF3	somite rostral/caudal axis specification	NM_008108	0.54	6.11E-12	0.4	1.80E-15	0.34	5.81E-17

CAPN1	protein autoprocessing	uc008ggj	0.54	4.93E-10	0.47	7.47E-12	0.47	4.85E-12
BMP4	mesenchymal cell differentiation involved in renal system development	NM_007554	0.56	4.63E-09	0.54	1.30E-09	0.4	5.22E-13
BDNF	negative regulation of neuroblast proliferation	NM_007540	0.56	1.84E-11	0.57	2.67E-11	0.6	1.37E-10
GLB1	galactose catabolic process	uc009rxj	0.58	2.61E-10	0.54	1.49E-11	0.54	1.62E-11
B3GALT4	protein glycosylation	NM_019420	0.59	4.93E-10	0.54	1.93E-11	0.6	5.05E-10
EXTL3	positive regulation of cell growth	uc007uuy	0.59	4.42E-09	0.5	1.87E-11	0.48	4.24E-12
TPST2	metabolic process	NM_009419	0.6	2.67E-10	0.5	1.09E-12	0.49	4.36E-13
GFPT2	glutamine metabolic process	NM_013529	0.6	8.06E-09	0.46	3.75E-12	0.17	3.22E-19
NCSTN	membrane protein ectodomain proteolysis	NM_021607	0.6	4.46E-06	0.65	3.59E-05	0.66	5.28E-05
SLC35E4	transmembrane transport	NM_153142	0.61	3.79E-09	0.6	2.04E-09	0.59	1.03E-09
IGFBP6	regulation of cell growth	NM_008344	0.61	1.32E-08	0.7	2.42E-06	0.71	2.64E-06
ACAN	collagen fibril organization	NM_007424	0.62	3.09E-08	0.45	1.93E-12	0.5	2.09E-11
ASGR2	regulation of protein stability	NM_007493	0.62	7.47E-07	0.54	6.83E-09	0.64	1.27E-06
MUC3	biological process	uc009abs	0.62	1.99E-09	0.6	2.87E-10	0.61	7.19E-10
CAPN1	protein autoprocessing	NM_007600	0.63	1.31E-07	0.56	2.85E-09	0.56	2.83E-09
ALG13	lipid glycolysation	uc009umu	0.63	1.21E-06	0.35	4.38E-13	0.21	1.21E-16
CLEC 10A	defense response	NM_010796	0.63	2.06E-08	0.61	4.11E-09	0.55	1.04E-10
EGFR	positive regulation of fibroblast proliferation	NM_207655	0.64	3.05E-06	0.48	7.84E-10	0.5	1.90E-09
WNT4	non-canonical Wnt receptor signaling pathway via MAPK cascade	NM_009523	0.64	1.35E-07	0.46	5.60E-12	0.6	9.70E-09
GMPPB	biosynthetic process	NM_177910	0.65	2.85E-09	0.6	9.28E-11	0.67	5.12E-09
GDF15	peripheral nervous system development	uc009mmb	0.65	5.10E-09	0.57	2.27E-11	0.58	4.47E-11
CHST 10	long term memory	NM_145142	0.65	9.75E-08	0.51	2.27E-11	0.63	1.44E-08
GNPDA1	fructose 6-phosphate metabolic process	NM_011937	0.66	1.22E-09	0.57	4.51E-12	0.52	1.32E-13
DHH	Leydig cell differentiation	NM_007857	0.66	6.74E-06	0.61	4.18E-07	0.63	1.37E-06
SULF2	glial cell-derived neurotrophic factor receptor signalling pathway	NM_028072	0.66	1.10E-05	0.6	2.92E-07	0.55	2.01E-08
FGF17	fibroblast growth factor receptor signaling pathway	NM_008004	0.67	3.08E-06	0.39	7.09E-13	0.46	2.79E-11
COG1	protein transport	NM_013581	0.67	1.54E-08	0.61	3.23E-10	0.57	1.91E-11
SLC35D1	carboxylic acid metabolic process	NM_177732	0.67	9.30E-08	0.63	5.70E-09	0.61	1.23E-09
GCNT2	metabolic process	uc007qen	0.68	2.22E-08	0.62	2.88E-10	0.66	2.90E-09
LGALS1	positive regulation of erythrocyte aggregation	NM_008495	0.69	1.64E-06	0.67	4.24E-07	0.57	1.58E-09
CHST12	dermatan sulfate biosynthetic process	NM_021528	0.69	5.84E-08	0.57	1.64E-11	0.53	1.67E-12
EXTL1	metabolic process	NM_019578	0.7	8.88E-06	0.71	1.09E-06	0.64	3.07E-07
DHH	Leydig cell differentiation	NM_007857	0.7	2.62E-06	0.69	1.13E-06	0.61	1.06E-08
FGFR1	middle ear morphogenesis	uc009lgc	0.7	5.35E-03	0.71	5.56E-03	0.47	5.68E-07
RFNJ	positive regulation of Notch signaling pathway	NM_009053	0.7	2.27E-06	0.65	8.94E-08	0.7	1.38E-06
CHPF	biological process	NM_001001566	0.71	2.55E-07	0.7	8.78E-08	0.68	2.24E-08

Table 1: Genes that were upregulated between all time-points of differentiating ESC versus Day 0. The top 75 transcripts, excluding housekeeping genes, are shown.

Down regulated genes	Biological process	Gen Bank Id	Day7 vs Day 0	Adj.P.Val	Day 10 vs Day 0	Adj.P.Val	Day 15 vs Day 0	Adj.P.Val
FGF8	mesodermal cell migration	NM_010205	42.3797232	1.01E-22	9.47508413	8.07E-19	5.11704525	2.54E-16
FGF5	signal transduction involved in regulation of gene expression	NM_010203	26.6249968	9.02E-20	11.68384194	1.97E-17	2.5661838	1.36E-09
CXCR4	positive regulation of oligodendrocyte differentiation	NM_009911	17.5585811	2.83E-21	10.6838942	6.47E-20	5.15100692	6.30E-17
FST	hair follicle morphogenesis	NM_008046	10.9455272	4.07E-17	4.6532678	1.53E-13	10.1117561	3.87E-17
GPC3	Positive regulation of BMP signalling pathway	NM_016697	9.26652576	1.59E-20	14.8298182	1.34E-22	12.9466229	3.72E-22
HAS2	cellular response to platelet-derived growth factor stimulus	NM_008216	7.70356913	2.80E-21	17.3878086	2.59E-24	5.40990498	4.71E-20
ST3GAL6	cellular response to interleukin-6	NM_018784	7.16222841	5.10E-16	4.82707743	3.02E-14	8.19634912	7.17E-17
PDGFRA	regulation of mesenchymal stem cell differentiation	NM_011058	6.15377193	3.87E-18	6.33145576	2.47E-18	20.8620143	8.22E-23
FGF10	positive regulation of urothelial cell proliferation	NM_008002	6.05568444	1.87E-18	3.48723842	2.25E-15	1.9503577	2.65E-10
BMP2	negative regulation of cardiac muscle cell differentiation	NM_007553	5.92915174	3.07E-16	9.3431268	2.47E-18	3.68169914	6.55E-14
TGFBR3	organ regeneration	NM_011578	5.84703718	8.68E-20	7.42068439	4.09E-21	11.6946987	5.37E-23
ST6GAL1	protien glycosylation	NM_145933	5.67294357	1.63E-19	4.34391694	3.15E-18	3.37249486	8.53E-17
WNT5A	positive regulation of interleukin-8 secretin	NM_009524	4.62657159	5.71E-16	5.21939383	1.14E-16	3.48696591	1.71E-14

ATRNL1	G-protein coupled receptor signaling pathway	NM_181415	4.37184806	5.20E-17	4.79796121	1.13E-17	4.7087415	1.01E-17
SLC35D3	carbohydrate transport	NM_029529	3.68726723	1.51E-13	3.39456334	4.01E-13	1.52523442	2.28E-05
BMP5	male genitalia development	NM_007555	3.45441937	4.42E-14	4.40143286	1.26E-15	2.90982973	4.49E-13
SHH	positive regulation of mesenchymal cell proliferation involved in urete development	NM_009170	2.84535026	2.97E-12	10.2782095	3.96E-19	7.52383004	4.87E-18
SULF1	glial cell derived neurotrophic factor receptor signaling pathway	NM_172294	2.8328506	1.61E-15	2.55258764	1.13E-14	1.8043247	6.04E-11
SMO	regulation of heart morphogenesis	NM_176996	2.70695189	2.48E-14	2.66693471	2.39E-13	2.16278874	1.90E-11
CHST1	keratin sulfate metabolic process	NM_023850	2.64294381	1.25E-10	2.91968655	1.51E-11	1.81412014	3.65E-07
IGFBP4	regulation of cell growth	NM_010517	2.59971141	2.04E-10	2.99138788	1.16E-11	5.92184608	6.04E-16
FZD1	canonical Wnt receptor signaling pathway involved in osteoblast differentiation	NM_021457	2.5929974	5.24E-11	4.22231948	1.47E-14	5.1629406	7.60E-16
PGM1	glucose metabolic process	NM_028132	2.54449087	4.62E-15	2.51157005	5.74E-15	3.82588695	2.40E-18
SRGN	maintenance of protease location in mast cell secretory granule	NM_011157	2.5281043	8.02E-07	9.04627559	1.15E-13	28.6174127	2.33E-17
IGFBP5	negative regulation of smooth muscle cell migration	NM_010518	2.52039135	1.33E-11	54.1924939	4.16E-24	49.0119677	1.49E-23
COLEC12	phagocytosis,recognition	NM_130449	2.50644878	1.07E-09	2.36517962	2.51E-09	1.76648989	1.85E-06
ACVR2B	embryonicforegut morphogenesis	NM_007397	2.49946961	1.76E-12	2.22216356	1.82E-11	1.61950818	1.12E-07
IL18	positive regulation of superoxide anion generation	NM_008360	2.49609567	5.57E-13	2.01655918	6.05E-11	1.75678725	2.73E-09
GAL3ST4	biosynthetic process	NM_001033416	2.45265361	1.64E-11	2.78469868	9.79E-13	1.81364832	1.61E-08
CXCL12	organ regeneration	NM_001012477	2.43638733	8.05E-14	2.3819499	6.16E-14	4.09876499	5.69E-18
GPC1	heparan sulfate proteoglycan catabolic process	NM_016696	2.41965101	8.35E-13	2.43278235	5.58E-13	1.88156515	2.85E-10
GPC6	heparan sulfate proteoglycan binding	NM_011821	2.37226306	5.03E-11	3.73767083	1.18E-14	6.05270893	1.96E-17
HES1	negative regulation of pro-B cell differentiation	NM_008235	2.33630154	1.61E-15	1.7039937	1.08E-11	1.64633452	2.96E-11
IGF1R	negative regulation of protein kinase B signaling cascade	NM_010513	2.32788291	2.37E-12	2.4505507	5.72E-13	2.64244098	9.13E-14
IGFBP4	regulation of cell growth	NM_010517	2.30803166	1.75E-09	2.49452869	2.43E-10	4.65968047	8.50E-15
HSPC159	biological process	NM_173752	2.28643633	2.50E-14	1.77978842	1.96E-11	1.51118941	6.90E-09
PAPSS1	3'-phosphoadenosine5'-phosphosulfate biosynthetic process	NM_011863	2.22345505	7.55E-12	3.00822711	1.20E-14	3.15825684	3.43E-15
GALNT12	carbohydrate metabolic process	NM_172693	2.2185426	3.07E-14	1.43576461	5.31E-08	1.56253689	1.13E-09
VEGFA	positive regulation of mesenchymal cell proliferation	NM_001025257	2.17808801	2.34E-08	4.54797309	8.33E-14	6.94702111	4.27E-16
NAGLU	middle ear morphogenesis	NM_013792	2.16817882	1.72E-12	3.3499713	2.65E-16	4.71733471	1.44E-18
PIGP	GPI anchor biosynthetic process	NM_019543	2.16685822	7.38E-14	2.20224463	3.69E-14	2.39139967	3.53E-15
FZD2	hard palate development	NM_020510	2.15852417	1.69E-14	3.68226121	4.69E-17	3.26765798	1.85E-16
GALNT10	protein O-linked glycosylation	NM_134189	2.1458266	8.17E-14	2.62941978	7.23E-14	2.18241959	3.27E-12
PIGP	GPI anchor biosynthetic process	uc008aak	2.1176694	4.20E-14	2.23027137	8.59E-14	2.41404614	9.41E-15
SLC35F1	transport	NM_178675	2.09359733	3.71E-09	2.90190844	3.07E-12	5.36672409	2.88E-16
PGM2L1	glucose metabolic process	NM_027629	2.07386145	7.84E-10	1.70134356	1.38E-07	1.42281342	4.37E-05
ARSA	binding of sperm to zona pellucida	NM_009713	2.04579877	5.44E-14	2.11042784	1.72E-13	1.88241796	3.19E-12
IGF2BP3	regulation of translation	NM_023670	2.03385031	7.89E-14	2.16576281	1.18E-14	1.75224985	4.19E-12
EXTL2	UDP-N-acetylgalactosamine metabolic process	NM_021388	2.02661107	5.57E-13	2.04072741	3.40E-13	1.92157761	1.39E-12
WNT11	adrenal gland development	NM_009519	1.99786452	7.49E-13	1.71547546	6.00E-11	2.70778888	2.92E-16
FUT11	protein glycosylation	NM_028428	1.99477254	1.94E-11	1.94396838	2.86E-11	1.73087405	8.54E-10
FZD7	substrate adhesion-dependent cell spreading	NM_008057	1.97598534	2.60E-12	1.87371495	9.43E-12	1.4459561	9.89E-08
BMP7	positive regulation of hyaluronone cable assembly	NM_007557	1.92125066	3.12E-12	2.01653612	6.05E-13	1.66673125	2.03E-10
LARGE	muscle cell homeostasis	NM_010687	1.91184823	2.29E-11	2.95378278	1.07E-15	2.13292577	6.51E-13
ACVR1	pharyngeal system development	NM_007394	1.89679598	1.31E-08	2.27486114	1.07E-10	2.89562597	6.23E-13
IGF2	insulin receptor signaling pathway via phosphatidylinositol3-kinase cascade	NM_010514	1.88169069	1.45E-13	6.1570209	8.38E-23	7.57795059	1.76E-23
GALNAC4S-6ST	hexose biosynthetic process	NM_029935	1.84870816	3.03E-11	2.01067722	1.99E-12	2.51071277	6.78E-15
B4GALNT2	lipid glycosylation	NM_008081	1.78603641	4.04E-05	8.15820522	8.20E-15	23.0281618	2.25E-18
FZD8	positive regulation of JUN kinase activity	NM_008058	1.77135361	8.82E-10	1.58880657	2.69E-08	1.64734018	5.78E-09
CHST2	N-acetylglucosamine metabolic process	NM_018763	1.73501904	3.47E-09	2.31786732	9.79E-13	4.08678333	3.29E-17
GPC2	neuron differentiation	NM_172412	1.71524689	4.26E-07	2.81062501	3.16E-12	2.97005519	8.86E-13
IGF2BP2	regulation of translation	NM_183029	1.70770941	4.09E-11	2.16833289	2.70E-14	2.15663684	2.18E-14
MAN2A2	mannose metabolic process	uc009iap	1.69900046	4.95E-09	2.06481819	1.21E-11	2.2423753	1.13E-12
GFRA2	nervous system development	NM_008115	1.68601544	2.05E-09	2.02091689	5.92E-12	1.4536158	3.43E-07
MDK	adrenal gland development	NM_010784	1.66964049	1.71E-10	2.06917008	1.63E-13	2.30332421	7.95E-15
ST8SIA4	ganglioside biosynthetic process	NM_009183	1.66846652	1.34E-07	2.80887175	3.01E-13	2.80100684	2.46E-13
FREM1	cell-matrixadhesion	NM_177863	1.66772539	1.44E-07	3.00801501	9.55E-14	4.51578012	1.38E-16
LMAN2L	protein transport	NM_001013374	1.65871958	3.15E-09	1.628116	4.41E-09	1.45645991	2.83E-07

ANGPTL2	signal transduction	NM_011923	1.64084049	2.31E-08	3.36741256	1.07E-15	3.62870614	1.76E-16
HES6	regulation of transcription from RNA polymerase II promoter	NM_019479	1.62914358	3.14E-08	1.55759132	1.26E-07	1.74304583	2.13E-09
POFUT1	fucosylation	NM_080463	1.62050504	1.05E-08	1.70715909	1.30E-09	1.76536807	3.63E-10
NAGA	glycolipid catabolic process	NM_008669	1.61677676	1.64E-09	1.9635424	2.06E-12	2.95211972	1.43E-16
FUT8	integrin-mediated signaling pathway	NM_016893	1.58474009	4.42E-08	2.21375951	1.71E-12	3.60985965	1.04E-16
NEU1	metabolic process	NM_010893	1.57773264	9.13E-09	2.67651596	3.94E-15	3.26914925	6.71E-17
HES6	regulation of transcription from RNA polymerase II promoter	NM_019479	1.55229634	7.83E-07	1.47541392	3.93E-06	1.53019762	8.60E-07

Table 2: Genes that were downregulated between all time-points of differentiating ESC versus Day 0. The top 75 transcripts, excluding housekeeping genes, are shown.

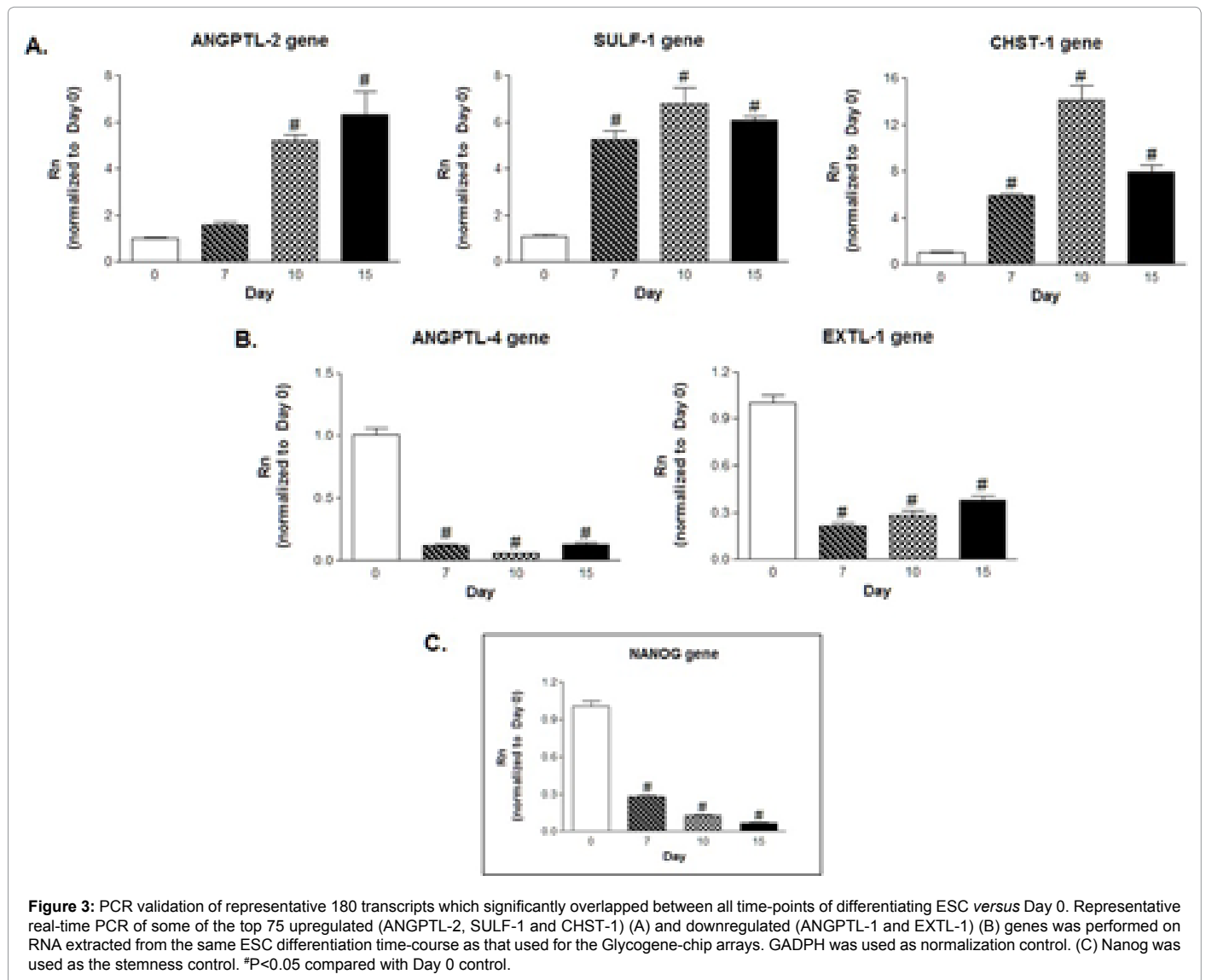


Figure 3: PCR validation of representative 180 transcripts which significantly overlapped between all time-points of differentiating ESC versus Day 0. Representative real-time PCR of some of the top 75 upregulated (ANGPTL-2, SULF-1 and CHST-1) (A) and downregulated (ANGPTL-1 and EXTL-1) (B) genes was performed on RNA extracted from the same ESC differentiation time-course as that used for the Glycogene-chip arrays. GAPDH was used as normalization control. (C) Nanog was used as the stemness control. *P<0.05 compared with Day 0 control.

(CHST-6, -10 and 12) were downregulated. Along with Table 1, this indicates that the latter family is strongly implicated in all facets of ESC differentiation, and demonstrates the pleiotropic functions imparted by various glyco-isoforms.

To validate some of the microarray results, 5 genes of interest were analyzed by real-time PCR, using the primer sequences depicted in Table 3. As such, we found that members of the Angiopoietin-like (ANGPTL) family, ANGPTL-2 and 4, were significantly regulated (Figure 3). ANGPTLs comprise a family of glycosylated cytokines

(ANGPTL-1 to -6) whose mechanisms of action and functions remain largely uncharacterized [30]. They are mainly located at sites of energy metabolism (liver and adipose tissues), vascular remodeling (uterus and ovaries) and inflammation. Although their roles in ESC *per se* remain largely unknown, a secondary role has recently emerged for ANGPTL-2 in promoting hematopoietic stem cell expansion [31,32]. PCR validation (Figure 3A) shows that ANGPTL-2 was upregulated by 5.2-fold at Day 10, persisting by Day 15 (6.3 fold). In stark contrast, ANGPTL-4 expression was downregulated immediately following

Gene	Forward Primer	Reverse Primer
ANG-1	CGGATTTCTCTCCAGAAAC	TCCGACTTCATATTTCCACAA
ANGPLT-2	CACCGTGAGGCATGTGAA	GGTTGGTCTTTATGAAGTAAAGC
ANGPLT-4	GGGACCTTAACGTGCCAAG	GAATGGCTACAGTACCAAAACC
ANGPLT-6	ATCTTCTCTGCTGCCACA	CGTGAGCCTCTGCACAATC
CHST-1	CCATCACAGGACCAGTTGAA	GCCTTCCAAGAACATTGCAT
EXTL-1	CAGGAGGTGGCAGGTTCTC	GCAGCTTCTCACTGTTCCAGA
GALNS	CTCCTGGGAGGAGTTCACAC	TGTAATCCTGAGACGTTCTGC
HS3ST-1	AGTGTGAATTTGCTCCAAAGG	GTATCTCCAGTTGCCAATTACTGA
NANOG	TTCTTGCTTACAAGGCTCTGC	AGAGGAAGGGCGAGGAGA
SULF-1	AAGAGTCACCTTCACCCCTTC	GCTH+GAAGTTTCTATCCACCTC
SDC-4	CCCTTCCCTGAAGTGATTGA	AGTTCCTGGGCTCTGAGG
GADPH	CCCAATGTGTCCGTCGTG	GCCTGCTTACCACCTTCT

Table 3: PCR primers used for real-time PCR experiments. GADPH represents the normalization gene. Nanog represents the stemness internal control gene.

differentiation, to almost null levels (Figure 3B). To our knowledge, this is the first report linking ANGPTL-4 and stem cells. Based on ANGPTL-4's proposed role as an angiogenic inhibitor, it's tempting to speculate that the balance between ANGPTL-2 and -4 might act as a switch to mediate stemness *versus* mesodermal differentiation [33]. Furthermore, recent studies have implicated a synergistic effect of the ANGPTL and IGF axes in promoting hematopoietic stem cell expansion [34]. In order to uncover more novel glycocones underlying ESC differentiation, we next focused on transcripts regulated to a lesser extent, but still having highly significant adjusted p values. We subjected the same ESC used for Glycogene-chip hybridization to PCR analysis, in order to eliminate any cell variability artefacts. As such, we found that the sulfatase, SULF-1, and the sulfotransferase, CHST-1, were highly upregulated as ESC differentiated, saturating at Day 10, whereas the glycosyltransferase exostosin (multiple)-like-1 (EXTL-1) was significantly downregulated (Figure 3A and 3B). Although the context of these transcripts in mediating ESC fate is unknown, studies using precursor stem cells have implicated a role for SULF-1 as a regulator of neural and hematopoietic differentiation [35,36]. Whereas there are no reports of CHST-1 expression in stem cells, in adult tissues, it is mainly expressed in neural and inflammatory tissues, where it modulates endothelium inflammation through glycosaminoglycan biosynthesis [37]. As for EXTL-1, a promoter of heparin sulfate chain elongation, it's preponderant role is as a tumor suppressor, which might explain its downregulation as ESC mature from the proliferating to the differentiating stage [38]. In order to confirm the stemness *versus* differentiation profile of our samples, we also subjected them to PCR analysis against the stemness marker, NANOG. As expected, NANOG transcripts decreased proportionally with time, achieving more than 70% downregulation at Day 7 and almost null expression after 10 and 15 days (87 and 93% decrease, respectively, Figure 3C).

A more detailed mechanistic analysis using the GeneGo Metacore software allowed us to identify possible biological networks modulated by these differentially expressed genes during all stages of ESC differentiation. The data was segregated into cellular compartments for added clarity. This type of analysis provides insight into physical connectivity and functional correlations between proteins. Although it would be interesting to validate these potential correlations in the future, it is not the scope of this study, but rather demonstrates that our methodology can be quickly analyzed in order to uncover not only potential glycome-related ESC signatures, but also underlying signaling mechanisms of action.

A top scoring network, using the transcripts from Table 1, revealed genes implicated in 5 main processes: (1) response to wounding (56.0%); (2) response to stress (72.0%); (3) nervous system development (60.0%);

(4) neurogenesis (52.0%) and (5) generation of neurons (50.0%) (Figure 4A). Highly connected nodes of interest included ANGPTL-2 and the transcription factor signal transducer and activator of transcription-3 (STAT-3), as well as and IGF-binding protein-2 (IGFBP-2, represented as IBP2 in the pathway) and the membrane glycoprotein integrin alpha-5 (ITGA-5). Although there is no documented record linking ANGPTL-2 and STAT-3, STAT-3 activation has been implicated in promoting neurogenesis [39], whereas the IGF-2/IBP-2/ITGA-5 axis promotes osteogenesis [40]. The CHST sulfotransferase family was found to be regulated in the cytoplasm, although its exact underlying mechanisms remain unclear, transcriptional activation downstream of the core-binding factor-1 (CBF-1) has been proposed to mediate neurogenesis [41].

A top scoring network, using the transcripts from Table 2, revealed genes implicated in 5 main processes: (1) carbohydrate metabolic process (40.0%); (2) N-acetylglucosamine metabolic process (16.0%); (3) glucosamine metabolic process (16.0%); (4) amino sugar metabolic process (16.0%) and (5) positive regulation of transcription during mitosis (12.0%) (Figure 4B). Highly connected nodes included FGF-4, PECAM and the CHST family, all with the transcription factor specificity protein-1 (SP-1). Although the link with CHST has not yet been demonstrated, transcriptional activation of FGF-4 or PECAM downstream of SP-1 has been shown to promote stemness [42] and vasculogenesis [43], respectively.

Likewise, we performed similar analyses on the 181 genes which were upregulated after 15 days (inclusive of Day 10) of ESC differentiation, in order to uncover glycocones implicated in the late differentiation stage. We focused on a lower scoring network in order to focus on non-developmentally conserved genes. In addition, the Venn diagram from Figure 1C indicated that this time-point has the largest number of differentially regulated transcripts, thus allowing us to unmask additional glycome-related signatures in differentiating ESC.

The underlying gene ontology analysis revealed 5 significantly grouped functional themes: (1) transferase activity; (2) transferase activity-transferring glycosyl groups; (3) cytokine binding; (4) receptor binding and (5) nucleic acid binding (Figure 5). As in the previous section, the IGF family was highly represented, with the most highly upregulated transcript being IGFBP-1 (191.80-fold, Table 4), underscoring the crucial role of this pathway in mediating all aspects of ESC fate. Interestingly, IGFBP-1 has been implicated in promoting liver regeneration [44]. The second and third most upregulated transcripts were proteoglycan family members, namely lumican (LUM, 45.43-fold) and decorin (DCN, 33.76-fold), which are both involved in promoting neurogenesis [45] and osteogenesis [46]. Investigating genes

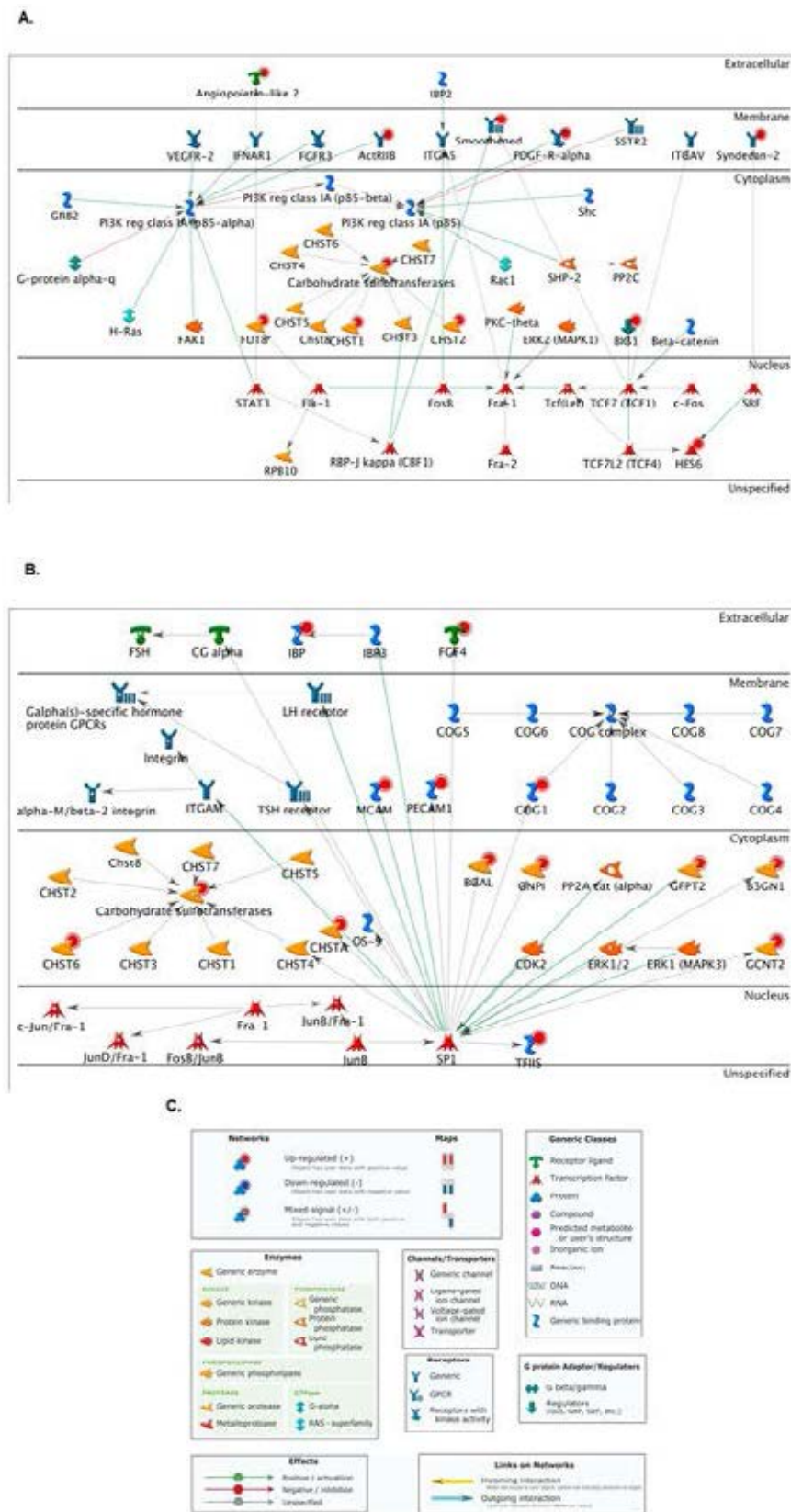


Figure 4: Network validation of the 180 transcripts which significantly overlapped between all time-points of differentiating ESC versus Day 0. A top scored biological pathway network of the upregulated (A) and downregulated (B) transcripts are represented, with the gene products segregated into their respective cellular compartments. These figures were created using the GeneGo Metacore software. The corresponding legend is represented in (C).

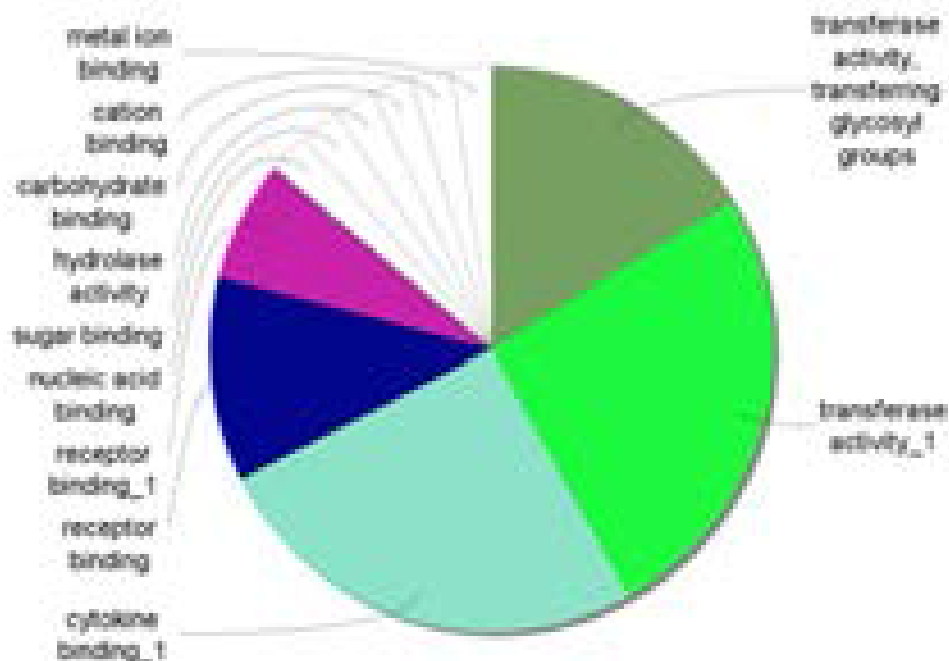


Figure 5: Classification of the 181 transcripts upregulated after 15 days of differentiation. Molecular functional annotation network overview chart of the 181 transcripts which were significantly upregulated after Day 15 of differentiation, inclusive of Day 10, which were created using ClueGO in Cytoscape.

biological process	Gen Bank ID	Fold Induction	Adj.P.Val
Insulin Receptor Signalling pathway	NM_008341	191.8	1.79E-19
response to growth factor stimulus	NM_008524	45.43	9.29E-17
peptide cross-linking via chondroitin4-sulfate glycosaminoglycan	NM_007833	33.76	3.22E-19
death	NM_025622	17.01	1.24E-17
metabolic process	NM_010474	15.06	5.69E-18
negative regulation of cell -substrate adhesion	NM_009262	11.98	5.75E-19
protein glycosylation	NM_009177	5.52	3.87E-17
memory gland morphogenesis	NM_009371	4.77	4.87E-18
regulation of cell differentiation	NM_010544	4.73	2.31E-15
negative regulation of apoptotic process	NM_009640	4.61	3.22E-19
trans membrane transport	NM_028060	4.4	6.40E-16
cell-cell adhesion	NM_016885	3.52	5.65E-16
germ cell migration	NM_021704	3.51	2.33E-17
negative regulation of mega karyocyte differentiation	NM_019932	3.14	1.58E-09
oligosaccharide metabolic process	NM_009181	3.02	2.09E-13
cell adhesion	NM_011693	2.97	3.86E-13
cell adhesion	NM_181277	2.9	3.00E-13
cell surface receptor linked signal transduction	NM_010550	2.84	1.85E-15
negative regulation of androgen receptor signalling pathway	NM_010512	2.83	4.62E-14
leukocyte tethering or rolling	NM_176973	2.82	3.00E-13
dephosphorylation	NM_001081306	2.8	2.87E-09
glial cell migration	NM_001081249	2.73	4.35E-14
embryo development	NM_173422	2.57	1.53E-13
apoptosis ans survival_Granzyme B signalling	NM_001017959	2.53	9.70E-14
cell-cell adhesion	NM_010740	2.48	1.47E-02
regulation of ERK1 and ERK2 cascade	NM_010207	2.44	2.59E-13
microphage chemotaxis	NM_009987	2.43	3.90E-06
glycolipid biosynthetic process	NM_011674	2.39	1.14E-10
response to methyl mercury	NM_009712	2.36	2.71E-12
cochlea development	NM_008010	2.3	8.01E-12
lipid glycosylation	NM_026247	2.27	7.74E-12

regualtion of cell growth	NM_018741	2.24	4.90E-08
positive regualtiopn of transcription,DNA- dependent	NM_009368	2.23	2.37E-09
cell proliferation	NM_001037859	2.19	1.41E-09
positive regulation of CD4-positive,alpha-beta T cell differentiation	NM_009856	2.14	4.36E-13
positive regulation of cell proliferation	NM_010419	2.09	2.50E-09
canonical Wnt receptor signalling pathway	NM_001042659	2.06	2.02E-10
Notch signalling pathway	NM_007865	2.05	4.19E-09
positive regulation of macrophage activation	NM_133775	2.03	1.86E-12
regulation of apoptotic process	NM_009370	2.01	2.86E-10
metabolic process	NM_015737	2.01	4.61E-10
lipid glycosylation	NM_008080	2	8.76E-11
cytokine-mediated signalling pathway	NM_008349	1.99	1.61E-11
defense response	NM_010739	1.98	4.06E-10
positive regulation of chemokine(C-X-C motif) ligand 2 production	NM_010545	1.94	2.99E-13
sphingolipid biosynthetic process	NM_019737	1.92	3.86E-13
positive regulation of cell proliferation	NM_013518	1.9	4.00E-10
regulation of mRNA stability involved in response to stress	NM_009951	1.9	1.66E-13
positive regualtion of T cell proliferation	NM_031252	1.86	2.27E-09
cell surface receptor signalling pathway	NM_019985	1.84	1.94E-09
germ cell programmed cell death	NM_021099	1.84	5.15E-10
angiogenesis	NM_145154	1.84	2.29E-09
organelle organization	NM_007693	1.83	7.02E-12
protein glycosylation	NM_009180	1.83	4.52E-10
glucose metabolic process	NM_175013	1.8	7.29E-09
decidualization	NM_001077184	1.77	3.35E-13
mannose metabolic process	NM_025837	1.71	9.91E-11
regulation of developmental process	NM_010929	1.71	1.65E-08
protein glycosylation	NM_011375	1.71	5.09E-13
neuropeptide signalling pathway	NM_010130	1.71	7.66E-04
galactose metabolic process	NM_016905	1.69	1.64E-10
inflammatory response	NM_145837	1.69	4.82E-12
positive regulation of transcription, DNA-dependent	NM_009612	1.68	5.67E-09
nerve maturation	NM_010017	1.67	1.17E-11
galactosylceramide catabolic process	NM_008079	1.67	2.13E-09
defense response	NM_010511	1.66	1.61E-08
skeletal system development	NM_007560	1.66	5.82E-08
fucosylation	NM_019934	1.66	1.52E-10
galactosylceramide biosynthetic process	NM_016922	1.65	1.17E-09
protein transport	uc009nqy	1.65	2.61E-11
proteinO-linked glycosylation via thronine	NM_139272	1.64	3.45E-10
metabolic process	NM_001033441	1.64	3.93E-09
growth	NM_145741	1.64	2.37E-10
metabolic process	NM_016722	1.64	6.15E-11
trmination of signal transduction	NM_011421	1.64	7.33E-10

Table 4: Genes that were downregulated after 15 days of differentiation *versus* Day 0. The top 75 transcripts, excluding housekeeping genes, are shown.

upregulated at this later differentiation time-point effectively allowed us to unmask novel glycogenes more readily than in the previous section. As such, top 10 regulated transcripts at Day 15 included heparan sulfate 3-O sulfotransferase HS3ST-1 (15.06-fold) and Angiopoietin-1 (ANGPT-1) (4.61-fold) (Table 4). We previously reported that another heparan sulfotransferase, NDST-1, is upregulated during the late stage of embryoid body differentiation, playing a preponderant role during vasculogenesis partly through the modulation of the IGF signaling axis [47]. Whether this is the case for HS3ST-1 remains to be determined, although knockout mice studies mainly suggest a role in clotting [48]. ANGPT-1, a glycosylated cytokine, is a potent promoter of both embryonic and adult angiogenesis, mainly through anti-apoptotic mechanisms downstream of its tyrosine kinase receptor, TIE-2 [49-51]. In stem cell settings, ANGPT-1 appears to promote survival of both endothelial and neural cells [52,53]. Interestingly, recent studies

have implicated a synergistic effect between ANGPT and IGF family members during angiogenesis and neurogenesis [54,55].

PCR validation of selected transcripts upregulated at Day 15 is shown in Figure 6, with ANGPT-1 and HS3ST-1 upregulated by 15.27- and 68.54-fold at Day 15, respectively. The importance of the ANGPTL family (Figure 3A and 3B) during ESC differentiation is reiterated here, as ANGPTL-6 transcripts were modestly but significantly upregulated (1.84-fold, Table 4) and PCR-validated (Figure 6). Although ANGPTL-6 mainly has a role as a glycosphingolipidsmodulator, in stem cell settings, it has been associated with hematopoiesis [56]. Interestingly, glycosphingolipids were recently shown to be important regulators of ESC differentiation into the endodermal and ectodermal lineages, partly through the upregulation of the glycosyltransferases beta-galactoside alpha-2,3-sialyltransferase-1 and -5 (ST3GAL-1 and ST3GAL-5) [57], which were upregulated by 5.52- and 1.71-fold

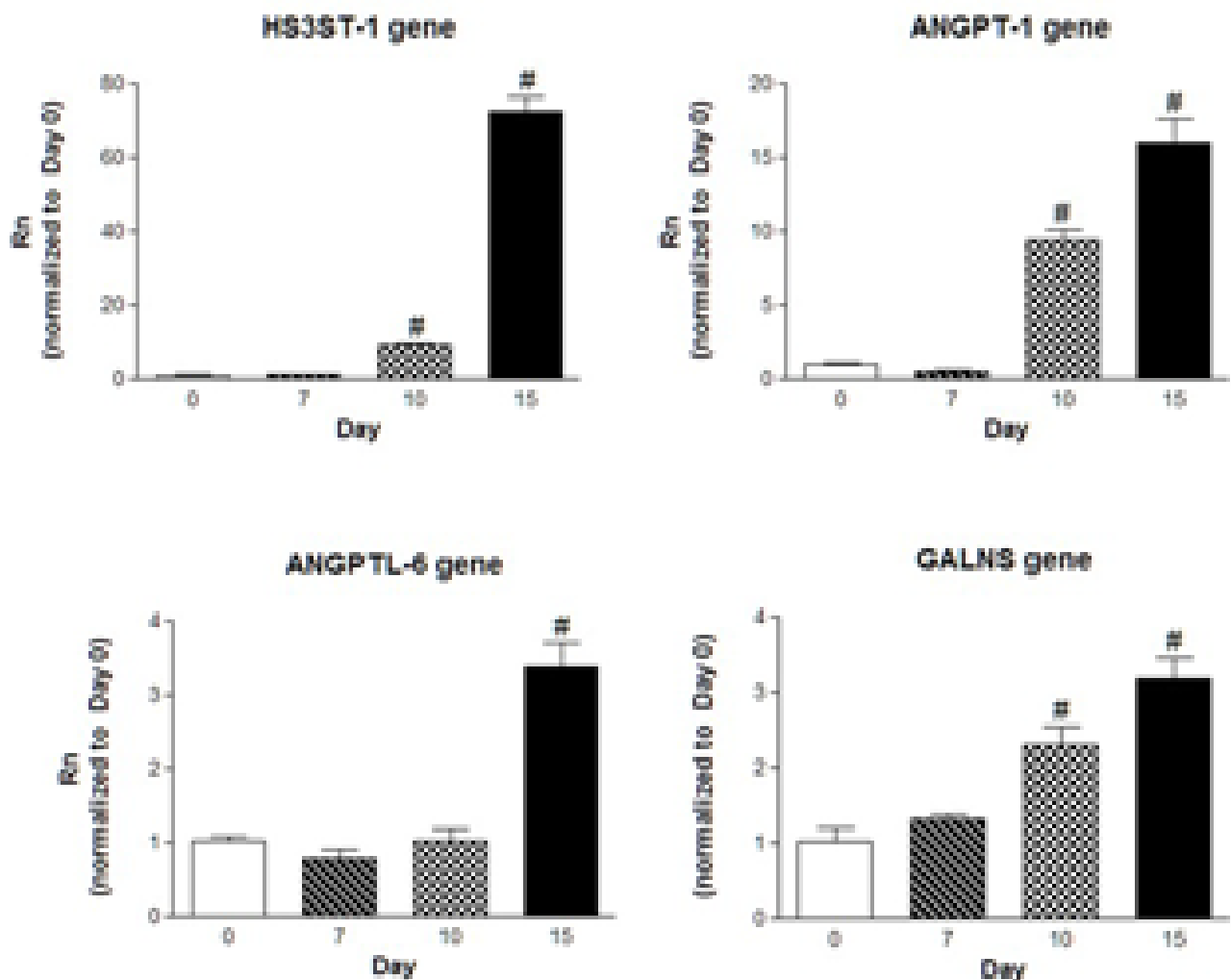


Figure 6: PCR validation of representative 181 transcripts which were significantly upregulated after 15 days of differentiation. Representative real-time PCR of some of the 75 upregulated genes, namely HS3ST-1, ANGPT-1, ANGPTL-6 and GALNS, was performed on RNA extracted from the same ESC differentiation time-course as that used for the Glycogene-chip arrays. GAPDH was used as endogenous control. *P<0.05 compared with Day 0 control.

in our study (Table 4). Whether there is a mechanistic link between ANGPTLs and ST3GALs during ESC differentiation, however, remains to be investigated. Combined with the other upregulated genes from Table 1, an interesting pattern is emerging. We have previously reported, using the Affymetrix GeneChip human genome array, that ANGPT-1 upregulates transcripts for ANGPTL-4 and CHSTs, while downregulating SULF-1 expression in endothelial cells [47]. It will be interesting to elucidate whether these transcripts are part of a novel pathway mediating vasculogenesis in the context of stem cell biology. In order to unmask an additional glycogene of interest, we looked at another modestly but statistically regulated gene, galactosamine (N-acetyl)-6-sulfate sulfatase (GALNS), which is involved in glycosaminoglycan degradation. GALNS was upregulated by 1.64-fold (Table 4) and PCR validated (Figure 6). GALNS transcripts are upregulated in response to FGF-2 during osteogenesis [58].

Metacore-generated biological pathway of these 181 genes revealed top scoring network implicated in 5 main processes: (1) regulation of sequence-specific DNA binding transcription factor activity (38.8%); (2) positive regulation of sequence-specific DNA binding transcription factor activity (32.7%); (3) positive regulation of cellular process

(75.5%); (4) positive regulation of response to stimulus (53.1%) and (5) positive regulation of biological process (77.6%). A highly connected node of interest included ANGPT-1/TIE-2 receptor and A20 binding inhibitor of NF-kappaB-2 (ABIN-2) (Figure 7A). Although the role of this axis in mediating ESC fate remains unclear, it's been shown to promote endothelial survival [59]. There were also links between the transcription factors STAT-3 and activator protein-1 (AP-1) with ANGPT-1. Whereas no link is known between AP-1 and ANGPT-1, STAT-3 (which was also correlated with ANGPTL-2 expression, Figure 4) has been implicated in mediating endothelial cell survival through the ANGPT-1/TIE-2 axis [60]. Mechanistic validation of Tie-2 protein activation using immunoblotting showed significant receptor phosphorylation after 7 days of differentiation (Figure 7B). It would be interesting in the future to investigate downstream mediators of the ANGPT-1/TIE2 axis in mediating ESC fate using Glycogene-chip hybridization in conjunction with Metacore analysis. Another interesting node included the forkhead transcription factor (FKHR) and vascular cell adhesion molecule-1 (VCAM-1). Our previous work has implicated FKHR as a mediator of vascularization during ESC differentiation [9].

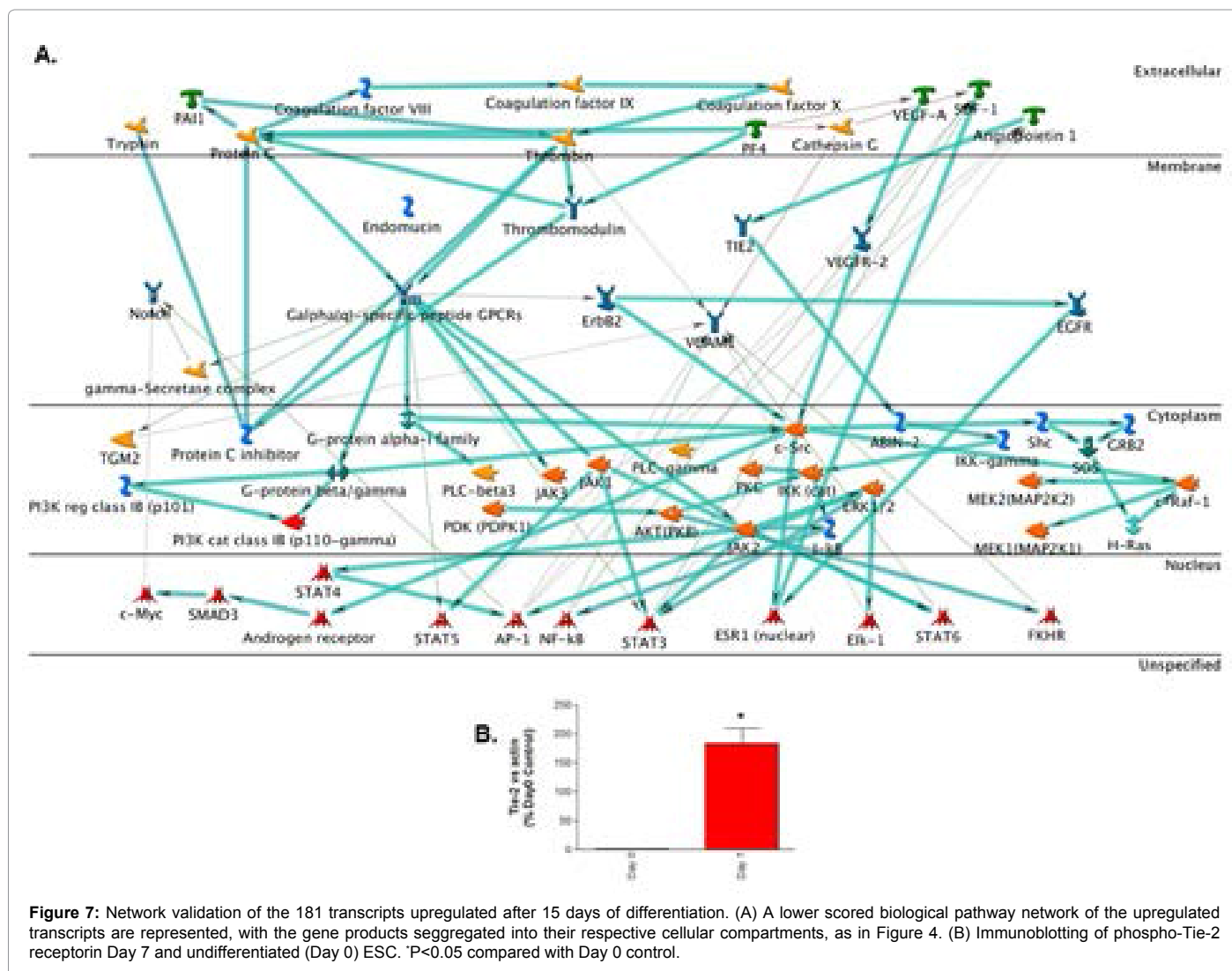


Figure 7: Network validation of the 181 transcripts upregulated after 15 days of differentiation. (A) A lower scored biological pathway network of the upregulated transcripts are represented, with the gene products segregated into their respective cellular compartments, as in Figure 4. (B) Immunoblotting of phospho-Tie-2 receptorin Day 7 and undifferentiated (Day 0) ESC. *P<0.05 compared with Day 0 control.

Taken together, the combination of the Glycogene-chip microarray with bioinformatic analyses in the embryoid body model gave us a rapid and reliable method for uncovering potential novel signaling mechanisms which mediate ESC fate. In addition, this methodology allowed us to uncover modestly regulated, but novel, glycogenes which would be masked using other methods.

Conclusion

In conclusion, our study demonstrates that combining the Glycogene-chip with a standard ESC-derived embryoid body model is a powerful screening method to uncover novel glycogenes signatures in differentiating *versus* cycling ESC. Aside from confirming the importance of growth factors/receptors such as the IGF, PDGF, TGF and FGF families, the integration of this method along with bioinformatic analyses and molecular biology tools (real-time PCR and immunoblotting) allowed us to uncover the potential involvement of novel glycogenes belonging to the Angiopoietin (ANGPT) and Angiopoietin-like (ANGPTL) families, as well as sulfotransferase, sulfatase and glycosyltransferase families. This study opens the door for future research to elucidate novel glycomic mechanisms which promote stemness *versus* differentiation. In turn, this would have profound implication for the regenerative medicine field.

Acknowledgement

The glycan analyses were performed by the Protein-Glycan Interaction Core (H) of the CFG, funded by NIGMS (GM62116). The authors wish to thank Mrs Lana Schaffer, Mrs Suzanne Papp and Mr Gilberto Hernandez at the Microarray Core of the CFG for their assistance with the microarray hybridization and ensuing analyses. We also thank Dr Zoltan Szabo and Dr Anne-Laure Papa for their editorial guidance. RH is supported by a CIHR postdoctoral fellowship. SS is supported by a National Institutes of Health Grant R01 (1R01CA135242-01A2) and a DOD grant (W81XWH-07-1-0482).

References

- Turnbull JE, Field RA (2007) Emerging glycomics technologies. Nat Chem Biol 3: 74-77.
- Haslam SM, Julien S, Burchell JM, Monk CR, Ceroni A, et al. (2008) Characterizing the glycome of the mammalian immune system. Immunol Cell Biol 86: 564-573.
- Rosenberg RD, Shworak NW, Liu J, Schwartz JJ, Zhang L (1997) Heparan sulfate proteoglycans of the cardiovascular system. Specific structures emerge but how is synthesis regulated? J Clin Invest 100: S67-S75.
- Rapraeger AC, Krufka A, Olwin BB (1991) Requirement of heparan sulfate for bFGF-mediated fibroblast growth and myoblast differentiation. Science 252: 1705-1708.
- Huang Z, Nelson ER, Smith RL, Goodman SB (2007) The sequential expression profiles of growth factors from osteoprogenitors [correction of osteoprogenitors] to osteoblasts in vitro. Tissue Eng 13: 2311-2320.

6. Sainz J, García-Alcalde F, Blanco A, Concha A (2011) Genome-wide gene expression analysis in mouse embryonic stem cells. *Int J Dev Biol* 55: 995-1006.
7. Tao SC, Li Y, Zhou J, Qian J, Schnaar RL, et al. (2008) Lectin microarrays identify cell-specific and functionally significant cell surface glycan markers. *Glycobiology* 18: 761-769.
8. Gao J, Liu D, Wang Z (2008) Microarray-based study of carbohydrate-protein binding by gold nanoparticle probes. *Anal Chem* 80: 8822-8827.
9. Harfouche R, Hentschel DM, Pieciewicz S, Basu S, Print C, et al. (2009) Glycome and transcriptome regulation of vasculogenesis. *Circulation* 120: 1883-1892.
10. Pieciewicz SM, Pandey A, Roy B, Xiang SH, Zetter BR, et al. (2012) Insulin-like growth factors promote vasculogenesis in embryonic stem cells. *PLoS One* 7: e32191.
11. Satomaa T, Heiskanen A, Mikkola M, Olsson C, Blomqvist M, et al. (2009) The N-glycome of human embryonic stem cells. *BMC Cell Biol* 10: 42.
12. Heiskanen A, Hirvonen T, Salo H, Impola U, Olonen A, et al. (2009) Glycomics of bone marrow-derived mesenchymal stem cells can be used to evaluate their cellular differentiation stage. *Glycoconj J* 26: 367-384.
13. Comelli EM, Head SR, Gilmartin T, Whisenant T, Haslam SM, et al. (2006) A focused microarray approach to functional glycomics: transcriptional regulation of the glycome. *Glycobiology* 16: 117-131.
14. Narayan S, Head SR, Gilmartin TJ, Dean B, Thomas EA (2009) Evidence for disruption of sphingolipid metabolism in schizophrenia. *J Neurosci Res* 87: 278-288.
15. Brown JR, Fuster MM, Whisenant T, Esko JD (2003) Expression patterns of alpha 2,3-sialyltransferases and alpha 1,3-fucosyltransferases determine the mode of sialyl Lewis X inhibition by disaccharide decoys. *J Biol Chem* 278: 23352-23359.
16. Smith FI, Qu Q, Hong SJ, Kim KS, Gilmartin TJ, Head SR (2005) Gene expression profiling of mouse postnatal cerebellar development using oligonucleotide microarrays designed to detect differences in glycoconjugate expression. *Gene Expr Patterns* 5: 740-749.
17. Lockhart DJ, Dong H, Byrne MC, Folletti MT, Gallo MV, et al. (1996) Expression monitoring by hybridization to high-density oligonucleotide arrays. *Nat Biotechnol* 14: 1675-1680.
18. Smyth GK (2004) Linear models and empirical bayes methods for assessing differential expression in microarray experiments. *Stat Appl Genet Mol Biol* 3: Article3.
19. Gentleman RC, Carey VJ, Bates DM, Bolstad B, Dettling M et al. (2004) Bioconductor: open software development for computational biology and bioinformatics. *Genome Biol* 5: R80.
20. Dezso Z, Nikolsky Y, Sviridov E, Shi W, Serebriyskaya T, et al. (2008) A comprehensive functional analysis of tissue specificity of human gene expression. *BMC Biol* 6: 49.
21. Bindea G, Mlecnik B, Hackl H, Charoentong P, Tosolini M, et al. (2009) ClueGO: a Cytoscape plug-in to decipher functionally grouped gene ontology and pathway annotation networks. *Bioinformatics* 25: 1091-1093.
22. Willems E, Mateizel I, Kemp C, Cauffman G, Sermon K, et al. (2006) Selection of reference genes in mouse embryos and in differentiating human and mouse ES cells. *Int J Dev Biol* 50: 627-635.
23. Vittet D, Prandini MH, Berthier R, Schweitzer A, Martin-Sisteron H, et al. (1996) Embryonic stem cells differentiate in vitro to endothelial cells through successive maturation steps. *Blood* 88: 3424-3431.
24. Leahy A, Xiong JW, Kuhnert F, Stuhlmann H (1999) Use of developmental marker genes to define temporal and spatial patterns of differentiation during embryoid body formation. *J Exp Zool* 284: 67-81.
25. Lake J, Rathjen J, Remiszewski J, Rathjen PD (2000) Reversible programming of pluripotent cell differentiation. *J Cell Sci* 113: 555-566.
26. Lange S, Heger J, Euler G, Wartenberg M, Piper HM et al. (2009) Platelet-derived growth factor BB stimulates vasculogenesis of embryonic stem cell-derived endothelial cells by calcium-mediated generation of reactive oxygen species. *Cardiovasc Res* 81: 159-168.
27. Fei T, Chen YG (2010) Regulation of embryonic stem cell self-renewal and differentiation by TGF-beta family signaling. *Sci China Life Sci* 53: 497-503.
28. Wu CY, Whye D, Mason RW, Wang W (2012) Efficient differentiation of mouse embryonic stem cells into motor neurons. *J Vis Exp*: e3813.
29. Choi SC, Choi JH, Park CY, Ahn CM, Hong SJ, et al. (2012) Nanog regulates molecules involved in stemness and cell cycle-signaling pathway for maintenance of pluripotency of P19 embryonal carcinoma stem cells. *J Cell Physiol* 227: 3678-3692.
30. Kim I, Moon SO, Koh KN, Kim H, Uhm CS, et al. (1999) Molecular cloning, expression, and characterization of angiopoietin-related protein. angiopoietin-related protein induces endothelial cell sprouting. *J Biol Chem* 274: 26523-26528.
31. Zhang CC, Kaba M, Ge G, Xie K, Tong W, et al. (2006) Angiopoietin-like proteins stimulate ex vivo expansion of hematopoietic stem cells. *Nat Med* 12: 240-245.
32. Broxmeyer HE, Srour EF, Cooper S, Wallace CT, Hangoc G et al. (2012) Angiopoietin-like-2 and -3 act through their coiled-coil domains to enhance survival and replating capacity of human cord blood hematopoietic progenitors. *Blood Cells Mol Dis* 48: 25-29.
33. Cazes A, Galaup A, Chomel C, Bignon M, Bréchet N, et al. (2006) Extracellular matrix-bound angiopoietin-like 4 inhibits endothelial cell adhesion, migration, and sprouting and alters actin cytoskeleton. *Circ Res* 99: 1207-1215.
34. Zhang CC, Kaba M, Izuka S, Huynh H, Lodish HF (2008) Angiopoietin-like 5 and IGFBP2 stimulate ex vivo expansion of human cord blood hematopoietic stem cells as assayed by NOD/SCID transplantation. *Blood* 111: 3415-3423.
35. Karus M, Denecke B, French-Constant C, Wiese S, Faissner A (2011) The extracellular matrix molecule tenascin C modulates expression levels and territories of key patterning genes during spinal cord astrocyte specification. *Development* 138: 5321-5331.
36. Langsdorf A, Do AT, Kusche-Gullberg M, Emerson CP Jr, Ai X (2007) Sulfs are regulators of growth factor signaling for satellite cell differentiation and muscle regeneration. *Dev Biol* 311: 464-477.
37. Nishimura M, Naito S (2007) Tissue-specific mRNA expression profiles of human carbohydrate sulfotransferase and tyrosylprotein sulfotransferase. *Biol Pharm Bull* 30: 821-825.
38. Kim BT, Kitagawa H, Tamura J, Saito T, Kusche-Gullberg M et al. (2001) Human tumor suppressor EXT gene family members EXTL1 and EXTL3 encode alpha 1,4-N-acetylglucosaminyltransferases that likely are involved in heparan sulfate/heparin biosynthesis. *Proc Natl Acad Sci USA* 98: 7176-7181.
39. Islam O, Loo TX, Heese K (2009) Brain-derived neurotrophic factor (BDNF) has proliferative effects on neural stem cells through the truncated TRK-B receptor, MAP kinase, AKT, and STAT-3 signaling pathways. *Curr Neurovasc Res* 6: 42-53.
40. Hamidouche Z, Fromigue O, Ringe J, Haupl T, Marie PJ (2010) Crosstalks between integrin alpha 5 and IGF2/IGFBP2 signalling trigger human bone marrow-derived mesenchymal stromal osteogenic differentiation. *BMC Cell Biol* 11: 44.
41. Mizutani K, Yoon K, Dang L, Tokunaga A, Gaiano N (2007) Differential Notch signalling distinguishes neural stem cells from intermediate progenitors. *Nature* 449: 351-355.
42. Lamb K, Rosfjord E, Brigman K, Rizzino A (1996) Binding of transcription factors to widely-separated cis-regulatory elements of the murine FGF-4 gene. *Mol Reprod Dev* 44: 460-471.
43. Gumina RJ, Kirschbaum NE, Piotrowski K, Newman PJ (1997) Characterization of the human platelet/endothelial cell adhesion molecule-1 promoter: identification of a GATA-2 binding element required for optimal transcriptional activity. *Blood* 89: 1260-1269.
44. Arai M, Yokosuka O, Fukai K, Imazeki F, Chiba T, et al. (2004) Gene expression profiles in liver regeneration with oval cell induction. *Biochem Biophys Res Commun* 317: 370-376.
45. Dellell M, Hu W, Papadaki V, Ohnuma S (2012) Small leucine rich proteoglycan family regulates multiple signalling pathways in neural development and maintenance. *Dev Growth Differ* 54: 327-340.
46. Burns JS, Rasmussen PL, Larsen KH, Schroder HD, Kassem M (2010) Parameters in three-dimensional osteospheroids of telomerized human mesenchymal (stromal) stem cells grown on osteoconductive scaffolds that predict in vivo bone-forming potential. *Tissue Eng Part A* 16: 2331-2342.
47. Abdel-Malak NA, Harfouche R, Hussain SN (2007) Transcriptome of

- angiopoietin 1-activated human umbilical vein endothelial cells. *Endothelium* 14: 285-302.
48. Moon AF, Xu Y, Woody SM, Krahn JM, Linhardt RJ, et al. (2012) Dissecting the substrate recognition of 3-O-sulfotransferase for the biosynthesis of anticoagulant heparin. *Proc Natl Acad Sci U S A* 109: 5265-5270.
49. Harfouche R, Hasséssian HM, Guo Y, Faivre V, Srikant CB, et al. (2002) Mechanisms which mediate the antiapoptotic effects of angiopoietin-1 on endothelial cells. *Microvasc Res* 64: 135-147.
50. Harfouche R, Gratton JP, Yancopoulos GD, Nosedá M, Karsan A, et al. (2003) Angiopoietin-1 activates both anti- and proapoptotic mitogen-activated protein kinases. *FASEB J* 17: 1523-1525.
51. Jeansson M, Gawlik A, Anderson G, Li C, Kerjaschki D, et al. (2011) Angiopoietin-1 is essential in mouse vasculature during development and in response to injury. *J Clin Invest* 121: 2278-2289.
52. Joo HJ, Kim H, Park SW, Cho HJ, Kim HS, et al. (2011) Angiopoietin-1 promotes endothelial differentiation from embryonic stem cells and induced pluripotent stem cells. *Blood* 118: 2094-2104.
53. Bai Y, Meng Z, Cui M, Zhang X, Chen F, et al. (2009) An Ang1-Tie2-PI3K axis in neural progenitor cells initiates survival responses against oxygen and glucose deprivation. *Neuroscience* 160: 371-381.
54. Nakamura K, Sasajima J, Mizukami Y, Sugiyama Y, Yamazaki M (2010) Hedgehog promotes neovascularization in pancreatic cancers by regulating Ang-1 and IGF-1 expression in bone-marrow derived pro-angiogenic cells. *PLoS ONE* 5: e8824.
55. Sivakumar V, Zhang Y, Ling EA, Foulds WS, Kaur C (2008) Insulin-like growth factors, angiopoietin-2, and pigment epithelium-derived growth factor in the hypoxic retina. *J Neurosci Res* 86: 702-711.
56. Fatrai S, van Gosliga D, Han L, Daenen SM, Vellenga E, et al. (2011) KRAS(G12V) enhances proliferation and initiates myelomonocytic differentiation in human stem/progenitor cells via intrinsic and extrinsic pathways. *J Biol Chem* 286: 6061-6070.
57. Liang YJ, Yang BC, Chen JM, Lin YH, Huang CL, et al. (2011) Changes in glycosphingolipid composition during differentiation of human embryonic stem cells to ectodermal or endodermal lineages. *Stem Cells* 29: 1995-2004.
58. Teplyuk NM, Haupt LM, Ling L, Dombrowski C, Mun FK, et al. (2009) The osteogenic transcription factor Runx2 regulates components of the fibroblast growth factor/proteoglycan signaling axis in osteoblasts. *J Cell Biochem* 107: 144-154.
59. Tadros A, Hughes DP, Dunmore BJ, Brindle NP (2003) ABIN-2 protects endothelial cells from death and has a role in the antiapoptotic effect of angiopoietin-1. *Blood* 102: 4407-4409.
60. Schubert SY, Benarroch A, Monter-Solans J, Edelman ER (2011) Primary monocytes regulate endothelial cell survival through secretion of angiopoietin-1 and activation of endothelial Tie2. *Arterioscler Thromb Vasc Biol* 31: 870-875.